Supplementary Information

High-energy all-solid-state lithium metal battery with "Single-crystal" Lithium-rich layered oxides

Xin Yin‡[ab], Deyang Li‡[ab], Liangwei Hao‡[ab], Yinzhong Wang[ab], Yongtao Wang[ab], Xianwei Guo*[ab], Shu Zhao[ab], Boya Wang[ab], Lingqiao Wu[ab], Haijun Yu*[ab]

a. Institute of Advanced Battery Materials and Devices, Faculty of Materials and Manufacturing, Beijing University of Technology, Beijing, 100124, P. R. China

b. Key Laboratory of Advanced Functional Materials, Ministry of Education, Beijing University of Technology, Beijing, 100124, P. R. China.

E-mail: hj-yu@bjut.edu.cn (H. Yu), xwguo@bjut.edu.cn (X. Guo).

‡ These authors contributed equally to this work.

Experimental section

Preparation of SC-LLOs cathode and garnet solid electrolyte

The SC-LLOs cathode materials were synthesized by the molten salt method that described in the previous work.[1] And the Ta-doped LLZO (LLZTO) powder with pure cubic phase structure was prepared by conventional solid-state sintering reaction.[2] For the fabrication of solid electrolyte pellet, the LLZTO powder was ball-milled and pressed into pellets in a 13 mm die at 350Mpa. Then the pellets were calcined at 1000 °C for 12h, following by the polish with sandpaper to remove the impurities on the surface and make the thin film of ~500 μm. The Li_3BO_3 (LBO) powder was prepared by the ball-milling process of LiOH and H_3BO_3 mixture with molar ratio of 1:3, and then sintered at 600 °C for 8h.

Preparation of composite cathode and ASSLMBs

For the HTXRD test, the composite material of SC-LLOs and LLZTO particles were mixed together (mass ratio of 1:1) and heated from 25 to 1000 °C, and then cooled down to 25 °C. The composite cathode composed of SC-LLOs+LLZTO with LBO additive was prepared by the co-sintering process at 700^{o}C for 1h,[3] in which the mass ratio of cathode and electrolyte materials were varied. The loading mass of SC-LLOs in the composite cathode is ~1.0 mg/cm^2. The composite cathode is prepared in the air by the co-sintering process, and the conductive carbon is not adopted. After making the composite cathode on the surface of LLZTO pellet, the opposite side was polished carefully. And the Li metal anode was prepared by the melting method on the surface of Au coated LLZTO pellet for making the good interface contact. The ASSLMBs with SC-LLOs+LLZTO+LBO/LLZTO/Li structure were assembled in an Ar-filled glovebox by using R2032 coin cell with nickel foam as current collector. For comparison, the liquid electrolyte based batteries

were assembled by the common method, and the electrolyte solution of 1.0 M $LiPF_6$ in EC: DEC=1:1 and R2032 coin cells with lithium foil were used.

Characterizations

The ionic conductivity of the LLZTO pellet was tested by Electrochemical Impedance Spectroscopy using Versa STAT 3 system at 25°C. The bulk resistance (R_b) was determined from the impedance spectrum that sandwiched between two stainless-steel (SS) plate electrodes and the spectra were recorded in the frequency range of 0.1 to 10^6 Hz with an AC amplitude of 10 mV. The ionic conductivity was calculated from equation: $\sigma = L/(R_bS)$, where L and S are the thickness and area of the LLZTO pellet, respectively. The electrochemical stability window was investigated by linear sweep voltammetry (LSV) performed on a working electrode of SS, LLZTO electrolyte and Li metal as the counter and reference electrode at a scan rate of 0.5 mV s^{-1} between -0.5 and 5.0 V. The *in-situ* high-temperature XRD was performed to check the interface reaction between SC-LLOs and LLZTO materials. The Bruker D8 Advance Diffractometer with Cu Kα radiation and a Ni filter were used. And the XRD patterns were collected on the same instrument from 10° to 80° at a scan rate of 4° min^{-1}. The details are as follows: The SC-LLO and LLZTO mixer with the mass ratio of 1:1 was detected in the temperature range of 25-1000 ºC. The heating rate is 100 ºC min^{-1} in the temperature range of 25-500 ºC, and the XRD patterns were collected every 100 ºC. In the range of 550-1000 ºC, the heating rate is 50 ºC min^{-1}, and XRD patterns were collected at each temperature for half an hour. After the heating process, the temperature naturally returned to 25 ºC, and the pattern was collected. The morphology and element distribution of composite cathode were collected by a field emission scanning electron microscope (SEM, Hitachi S-4800) with an energy-dispersive X-ray scattering system. The Electrochemical Impedance Spectroscopy of ASSLMBs

was collected by using Versa STAT 3 system at 80°C. The resistances were determined from the impedance spectrum that sandwiched between two stainless-steel (SS) plate electrodes and the spectrum was recorded in the frequency range of 0.1 to 10^6 Hz with an AC amplitude of 10 mV. The impedance spectrum was analyzed using ZView Software. For the equivalent circuit, the R0 is the internal resistance for the solid-state battery, CPE is the element with constant phase angle, W is the Warburg impedance, and the R1 and R2 are the interfacial charge transfer resistances for the anode and cathode side. To examine the structure change after cycling, the solid batteries were disassembled in the glove box, and the composite cathode was collected.

Electrochemical measurements

The ASSLMBs were assembled in an Ar-filled glove box. And the batteries were charged and discharged between 2.0 and 4.7 V at the current density of 0.05C at 80℃ (1C=200 mAh g^{-1}). The current density and the specific capacity were calculated based on the mass of SC-LLOs in the composite cathode. The galvanostatic charge/discharge tests of CR2032 were conducted on LAND testing system (Wuhan LAND electronics Co., Ltd.). The liquid electrolyte based battery was tested with the same conditions at 25°C.

Theoretical Calculations

All the calculations were performed using spin-polarized DFT methods implemented in the VASP code Projector augmented wave (PAW) method was used to describe the interactions between the ions and valence electrons[4-6]. The exchange-correlation interactions of valence electrons were calculated via the generalized gradient approximation (GGA) in the Perdew-Burke-Ernzerhof (PBE) form[7]. The cutoff energy was set to 450 eV, whereas the Brillouin zone was sampled at the Γ-point. DFT+*U* calculations with a value of U_{eff} = 4.0 eV for Zr 4*d* state was applied to correct the strong

electron-correlation properties of ZrO_2[8-10]. The convergence criteria for the electronic self-consistent iteration and force were set to 10^{-4} eV and 0.02 eV/Å, respectively.

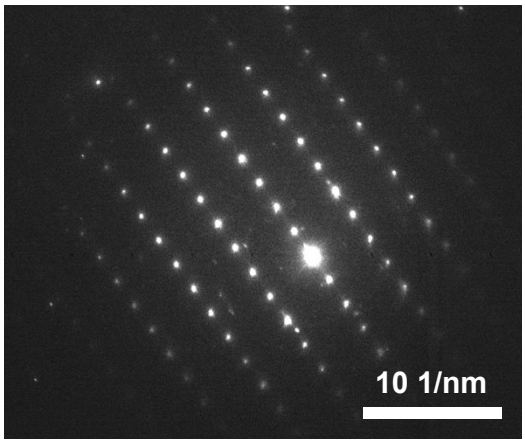

Fig. S1 The selected electron diffraction pattern of the SC-LLOs cathode material.

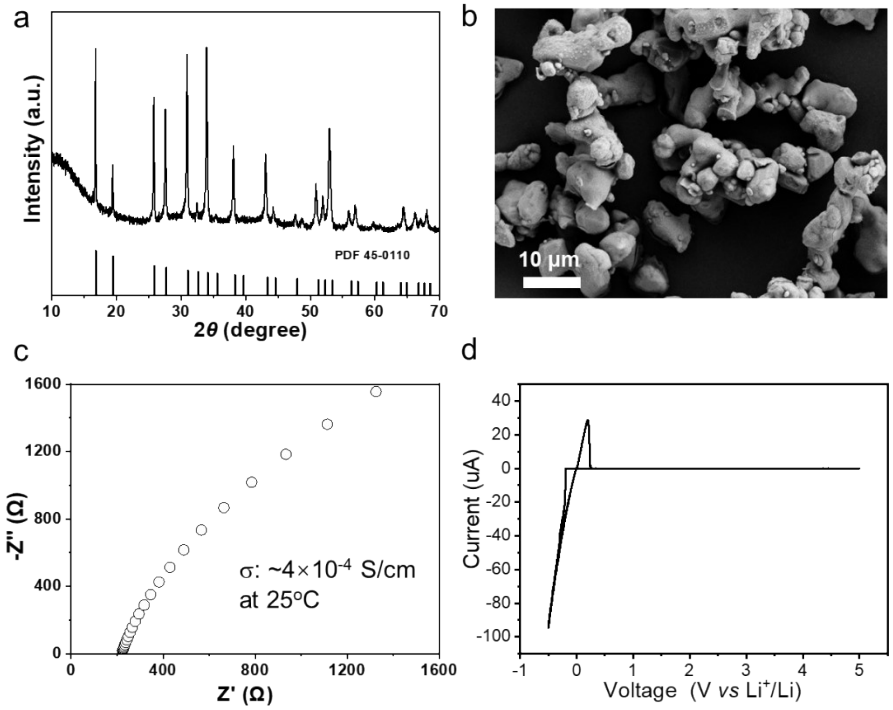

Fig. S2 The (a) XRD pattern and (b) SEM image of LLZTO solid electrolyte powder. The (c) EIS and (d) LSV of LLZTO solid electrolyte pellet. The scan rate for the LSV is 0.5 mV/s.

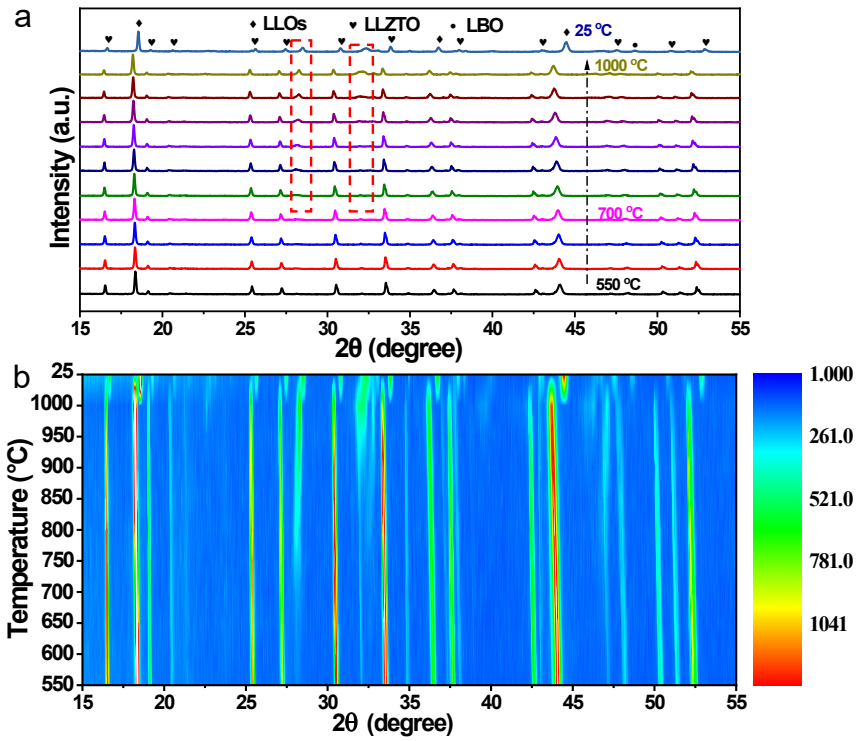

Fig. S3 The (a) *in-situ* XRD patterns with the appearance of new phase, and (b) the corresponding full contour plot of 2D XRD patterns for *in-situ* HTXRD from 550 to 1000 °C and cooling down to 25°C.

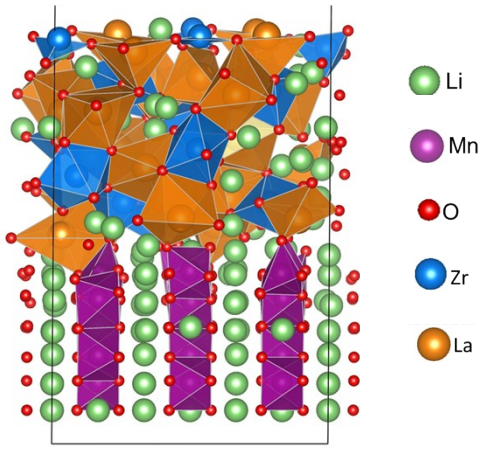

Fig. S4 The interface model of Li_2MnO_3 (010)/LLZO(100).

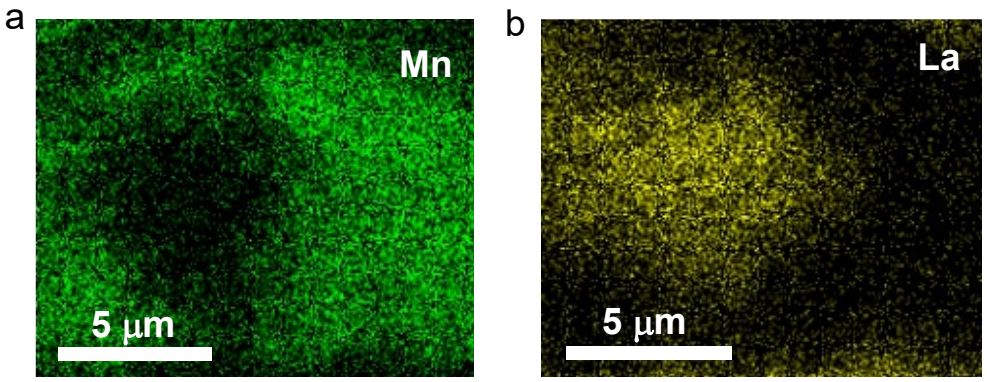

Fig. S5 The Mn element and (b) La element mapping in the composite cathode after co-sintering.

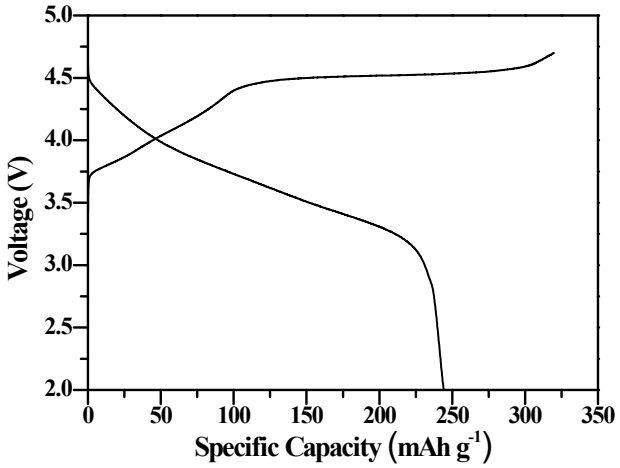

Fig. S6 The initial charge/discharge curves of liquid electrolyte based battery with SC-LLOs cathode material between 2.0 and 4.7 V.

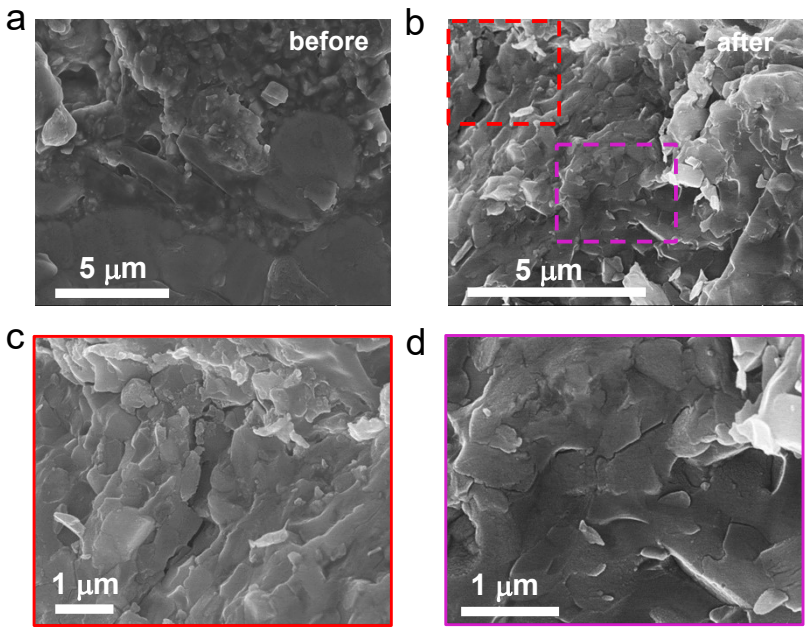

Fig. S7 The SEM images of composite cathode (a) before and (b) after cycling. (c-d) The enlarged parts for the cracks that mraked in (b).

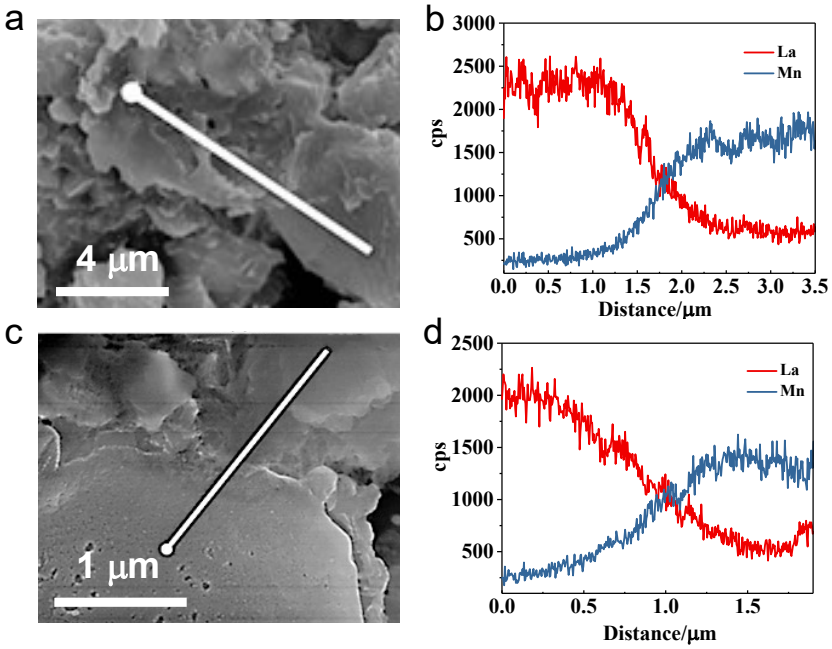

Fig. S8 The interdiffusion of Mn and La elements in the interface of composite cathode before and after cycling.

Table S1 The cell parameters in crystal structure of SC-LLOs cathode material.

Space group	Cell parameters			Ratio	Structure
	a	b	c		
C2/m	4.9403(3) Å	8.5467(5) Å	5.0286(4) Å	55.96%	$Li_{1.2}Mn_{0.567}Ni_{0.167}Co_{0.067}O_2$
R-3m	2.85321(5) Å	2.85321(5) Å	14.2318(6) Å	44.04%	

Table S2 The molar ratio of Ni/Co/Mn elements in the SC-LLOs cathode material.

	Molar ratio of transition metal elements		
	Mn	**Ni**	**Co**
Theoretical	0.567	0.167	0.067
Experimental	0.548	0.173	0.079

Table S3 The comparisons of discharge capacities in garnet-based ASSLMBs with the sintered or blended composite cathodes, which including the $LiFePO_4$, $LiNi_xCo_yMn_{1-x-y}O_2$, and $LiCoO_2$ cathode materials.

Configuration of all-solid-state battery	Temper-ature	Current density	Voltage Range (V)	Initial discharge capacity (mAh/g)	Cycles	Final discharge capacity (mAh/g)	Ref.
NCM622+LBO+LLZTO /LLZO/Li	80°C	0.05 C (1C=180 mA/g)	2.8-4.3	138.8	50	79	21
NCM811+LBO+Ta-LLZO /Ta-LLZO/Li	60°C	40 μA /cm^2	3.0-4.2	120	30	70.8	22
NCM523+LBO+ITO /LLZTO/Li	80 °C	5 μA/cm^2	3.0-4.6	123.3	5	76.6	13
LCO+LBO+ITO /LLZO /Li	80°C	0.1 C (1C=140 mA/g)	3.0-4.5	116	50	64	14
LCO+LLZNO+γ-ALO /LLZNO/Li	RT	0.2 C (1C=137 mA/g)	2.8-4.15	55.6	160	55.6	15
LCO+LBO+ITO /LLZTO/Li	80°C	5 μA/cm^2	2.8-4.3	69.6	1	69.6	16
LCO+LBO+LLZO /LLZO/Li	80°C	14 μA/cm^2	3.0-4.1	101	40	67	17
LCO+LBOCl+LLZTO /LBOCl+LLZTO/Li	90°C	0.05 C	3.0-4.1	93.8	50	~ 69	18
LCO+AlO /LLCZTO/Li	30°C	3.85 μA/cm^2	2.5-4.2	90	100	76.5	19
LCO+LLZTO+LCBO /LLZTO/Li	100°C	0.05 C (1C=115 mA/g)	3.0-4.05	106	40	67	20
LFP+LLZTO /BN+LLZTO/Li	60°C	100 μA/cm^2	2.8-4.4	120.94	100	119	12
SC-LLOs+LBO+LLZTO /LLZTO/Li	80°C	0.05 C (1C=200 mA/g)	2.0-4.7	226	30	180	This work

References

1. Y. Wang, L. Wang, X. Guo, T. Wu, Y. Yang, B. Wang, E. Wang and H. Yu, *ACS applied materials & interfaces*, 2020, **12**, 8306-8315.
2. D. O. Shin, K. Oh, K. M. Kim, K. Y. Park, B. Lee, Y. G. Lee and K. Kang, *Sci Rep*, 2015, **5**, 18053.
3. X. Guo, L. Hao, Y. Yang, Y. Wang, Y. Lu and H. Yu, *Journal of Materials Chemistry A*, 2019, **7**, 25915-25924.
4. G. Kresse and J. Furthmüller, *Computational Materials Science*, 1996, **6**, 15-50.
5. J. P. Perdew, K. Burke and M. Ernzerhof, *Phys Rev Lett*, 1996, **77**, 3865-3868.
6. B. Chen, I. A. Meinertzhagen and S. R. Shaw, *J Comp Physiol A*, 1999, **185**, 393-404.
7. D. G. Barnes, M. Vidiassov, B. Ruthensteiner, C. J. Fluke, M. R. Quayle and C. R. McHenry, *PLoS One*, 2013, **8**, e69446.
8. F. Twisk, *J Rehabil Res Dev*, 2013, **50**, vii-viii.
9. D. Chen, K. P. Taylor, Q. Hall and J. M. Kaplan, *Genetics*, 2016, **204**, 1151-1159.
10. Y. Tang, S. Zhao, B. Long, J.-C. Liu and J. Li, *The Journal of Physical Chemistry C*, 2016, **120**, 17514-17526.